

Heterogeneous Sparse Matrix-Vector Multiplication via Compressed Sparse Row Format

Phillip Allen Lane^{1,*}, Joshua Dennis Booth²

Abstract

Due to ill performance on many devices, sparse matrix-vector multiplication (SpMV) normally requires special care to store and tune for a given device. However, SpMV is one of the most important kernels in high-performance computing (HPC), and therefore, a storage format and tuning are required that allows for efficient SpMV operations with low memory and tuning overheads across heterogeneous devices. Additionally, the primary users of SpMV operations in HPC are normally application scientists that already have numerous other libraries they depend on the use of some standard sparse matrix storage format. As such, the ideal heterogeneous format would also be something that could easily be understood and requires no major changes to be translated into a standard sparse matrix format, such as compressed sparse row (CSR). This paper presents a heterogeneous format based on CSR, named CSR- k , that can be tuned quickly, requires minimal memory overheads, outperforms the average performance of NVIDIA's cuSPARSE and Sandia National Laboratories' KokkosKernels, while being on par with Intel MKL on our test suite. Additionally, CSR- k does not need any conversion to be used by standard library calls that require a CSR format input. In particular, CSR- k achieves this by grouping rows into a hierarchical structure of super-rows and super-super-rows that are represented by just a few extra arrays of pointers (i.e., < 2.5% memory overhead to keep arrays for both GPU and CPU execution). Due to its simplicity, a model can be tuned for a device, and this model can be used to select super-row and super-super-rows sizes in constant time. We observe in this paper that CSR- k can achieve about 17.3% improvement on an NVIDIA V100 and about 18.9% improvement on an NVIDIA A100 over NVIDIA's cuSPARSE while still performing on-par with Intel MKL on an Intel Xeon Platinum 8380 and an AMD Epyc 7742.

1. Introduction

Sparse matrix-vector multiplication (SpMV) has remained one of the most important kernels in high-performance computing (HPC) due to its use in applications such as machine learning and iterative solvers (e.g., Conjugate Gradient (CG) and GMRES for partial differential equations (PDEs)) [13]. Modern systems are composed of numerous heterogeneous compute units, e.g., many-core CPUs, GPUs, and FPGAs. Each of these compute units have different microarchitecture properties that influence how they access and process data. Due to SpMV's importance and shift in system design, a need exists for a heterogeneous format, i.e., a data structure that can be efficiently utilized by different compute units, for SpMV. This SpMV format needs to exist so that it requires only minor adjustments and minimal storage overheads, so as to not incur unnecessary and further demand on the memory subsystem. Overall, the problem of constructing such a format is difficult. Even on many-core systems, optimizing the performance of SpMV requires tuning given the sparse matrix, microarchitecture of the hardware, and the number of SpMV operations the application will execute [14, 19, 22]. Optimizing on accelerators, such as GPUs, can be even more difficult and many of the optimization

choices utilized for many-core systems, such as blocking and base format, are completely different. In this work, we propose extending the well-known many-core system CSR- k [14, 15] format to be heterogeneous for both parallel many-core systems and GPUs as this format is both flexible enough and compatible with many already standard interfaces that utilize CSR format.

SpMV, i.e., $Ax = y$ where A is a sparse coefficient matrix and x, y are dense vectors, is well-known to be a notoriously difficult kernel to optimize because of its memory bandwidth requirements [6, 11, 19]. The primary challenge in optimizing SpMV is its relatively poor performance on devices due to low computational intensity, i.e., the number of floating-point operations per memory load is low. Recalling the general algorithm for SpMV, for each row (i) of A the nonzero elements are multiplied by their corresponding elements in x and added together for a single element in y (y_i). Each of these nonzeros in a row results in three loads (i.e., $a_{i,j}$, x_j , and y_i) and one store must occur per multiply-add operation. Additionally, there exists little data reuse as each $a_{i,j}$ is only used once and y_i is only used for each row. Making matters even more difficult, the one array that does see reuse (i.e., x) might be accessed effectively at random, depending on the structure of the matrix. This makes it extremely difficult for cache structures to consistently hold relevant data, and places SpMV firmly on the bandwidth-limited roofline of the roofline model [26]. Figure 1 sketches the roofline model for the GPU NVIDIA Ampere A100, following the observations of [18] and our data in Section 6. Oftentimes, SpMV may only see a small fraction of the peak performance of a compute

*Corresponding author

Email addresses: phillip.lane@uah.edu (Phillip Allen Lane), joshua.booth@uah.edu (Joshua Dennis Booth)

¹Graduate Student

²Assistant Professor of Computer Science

device (often around 10%) because a very proportionally large amount of time is spent waiting for memory access [17].

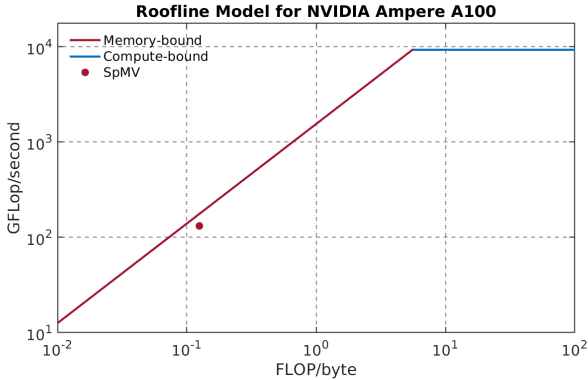


Figure 1: An example roofline model for GPUs for the NVIDIA Ampere 100. SpMV is restricted by its low arithmetic intensity, and hence low FLOP/s.

Currently, SpMV formats such as coordinate list (COO) and compressed sparse row (CSR) [12, 21] are used to reduce the memory overhead of storing sparse data. This reduction aids large sparse matrices to better fit into the main memory and may reduce the number of loads needed to keep data in higher cache levels. However, they are not designed in consideration of parallel processing and the complex microarchitecture of modern devices, such as nonuniform memory accesses (NUMA) on many-core systems. A second challenge is the complexity of the optimization. This complexity comes in the forms of the time to optimize and overhead in the size of the data structure. For example, the process of autotuning SpMV was popular in the early 2000s [1, 22], and the cost for tuning SpMV on many-core systems by constructing complex multi-level block structures could be amortized over the length of the application. However, both the computational device and the number of concurrent threads could theoretically change per iteration of the application in modern heterogeneous systems, and the cost of autotuning would be too high on such systems.

Therefore in this paper, we extend CSR-*k* for heterogeneous systems. This extension has the following significant benefits. The first is that CSR-*k* has a very small storage overhead compared to CSR. Since CSR-*k* is an extension of the CSR format, we analyze the overhead of additional storage and find that the overhead is always $< 2.5\%$. Secondly, the format is easy to understand by application scientists as it does not require bit-level indexing or specialized hash tables (unlike other heterogeneous SpMV formats [3, 19]). As such, it is easy to integrate into existing codes and visualization software. This is important for computational scientists looking to convert their CSR-based kernels to CSR-*k*-based kernels. Lastly, the tuning time is far smaller than other methods (e.g., pOSKI [1, 22]) as the parameter space is much smaller, and, as we observe in the paper, the tuning can be done in constant time after training a simple model.

This paper provides the extension of CSR-*k* for heterogeneous systems, in particular CPUs and GPUs, in the following manner:

- An overview of the implementation changes needed for CSR-*k* on NVIDIA GPUs
- The first model-driven selection of tuning parameters for the CSR-*k* format to provide constant-time parameter selection
- A comparison of CSR-*k* to KokkosKernels [10] and NVIDIA’s cuSPARSE on Volta V100 and Ampere A100
- A comparison of the impact of sparse matrix band re-ordering on performance
- A comparison of CSR-*k* to Intel MKL on Xeon Platinum 8380 and Epyc 7742
- An analysis of overheads for CSR-*k*

2. Background and Related Work

In this section, we present some of the most common implementation formats for SpMV on CPU and CPU/GPU heterogeneous formats. Through this presentation, we outline the strengths and weaknesses of each and the current state.

2.1. Formats for CPU

Though many SpMV formats have been studied [9, 12, 14, 21, 23, 24], two standard formats have become popular for SpMV due to reducing memory overheads and their relative ease of understanding, i.e., Coordinate list (COO) and Compressed Sparse Row (CSR). COO is the most straightforward format for storing a sparse matrix. The COO format contains three arrays (i.e., `col_idx`, `row_idx`, and `vals`) each array is the length of the number of nonzeros (NNZ) in the sparse matrix. However, several drawbacks exist for utilizing COO on many-core systems. These drawbacks include the overall storage required is $3 \times NNZ \times 32$ bits if we consider 32 bit integers and single-precision floating-point values, and the format itself does not provide any ordering of how the nonzero values should be processed. As a result, a SpMV of a sparse matrix that is stored in COO based on a random permutation of `col_idx` and/or `row_idx` would have poor performance, and lock or atomic operations would be needed for parallel implementations.

CSR is designed to be a more space-efficient data structure than COO. It does this by blocking nonzero elements into shared rows. The format contains three arrays (i.e., `row_ptr`, `col_idx`, and `vals`). The `row_ptr` array provides the running cumulative sum of the nonzero elements in each row and hence has size $m + 1$ for an $m \times n$ sparse matrix. The `col_idx` provides the column index and the `vals` provides the values for each of the nonzero elements. As such, the CSR requires $(2 \times NNZ + m + 1) \times 32$ bits of data. Figure 2 provides an example of this format in black (ignoring SR and SSR).

Sparse blocked based formats, such as Block Compressed Sparse Row (BCSR) [9, 24] or Unaligned Block Compressed Sparse Row [23], take the idea of CSR into a second dimension. Nonzero elements are grouped together in two-dimensional blocks

Row									SR	SSR
0	1	8							0	0
1		9	5	3						
2		1	3	8	5				1	
3				2						
4				2	3	6				
5					7	9			2	1
6						9	6			
7				4	5	3	6		3	
8						9	8	3		

```

vals = { 1, 8, 9, 5, 3, 1, 3, 8, ... }
col_idx = { 0, 1, 1, 2, 3, 1, 2, 3, ... }
row_ptr = { 0, 2, 5, 9, 10, 13, 15, ... }
sr_ptr = { 0, 2, 5, 7, 9 }
ssr_ptr = { 0, 2, 4 }

```

Figure 2: Example of the CSR-3 data structure with the super-row pointer (`sr_ptr`) and super-super-row pointer (`ssr_ptr`). Super-rows and super-super-rows are shown to the right of the matrix.

that are normally dense. Many sparse matrices from finite-element analysis often exhibit this dense block substructure. These blocks are next grouped together in some outer blocking structure, such as by row in BCSR. These can be highly optimized due to the number of different parameters they provide, e.g., the number of rows and columns in a block. However, the performance of BCSR depends on grouping together nonzero elements into a block. Though these formats can reduce the memory needed to store the sparse matrix, the true advantage of these formats is having smaller structures and memory access patterns that better fit the hierarchical cache memory structures in many-core systems. In particular, these small dense blocks can better fit into L1 or L2 caches.

In the application space, SpMV formats are hard to separate from reorderings. Sparse reorderings permute nonzero elements, and these reorderings can provide better memory accesses [7], improve iteration counts of sparse iterative solvers [2], and can provide better groupings of nonzeros, such as those taken advantage of by many block based formats and supernodes in sparse direct methods. An example of these reorderings include reorderings that reduce the band around the diagonal, i.e., reorderings that pull nonzero elements toward the diagonal, such as spectral reorderings [4] and Reverse Chuthill-McKee (RCM) [7]. Therefore, it is almost always the case that some reordering is applied to the sparse matrix in conjunction with selecting a storage format.

2.2. CSR- k

One CSR based format that has shown to greatly improve parallel performance and be more aware of the hierarchical cache structure is CSR- k [14, 15]. CSR- k is a multilevel data structure for storing sparse matrices based on CSR. This format utilizes both multilevel structures that better fit the cache structure of many-core systems and multiple levels of reorderings to reduce the envelope or band size for a level. In particular, the k represents a small integer ≥ 2 that defines the number of ad-

Listing 1: SpMV-3 CPU kernel

```

1  function SpMV_3(num_ssr, ssr_ptr[],
2      sr_ptr[], r_ptr[], col_idx[],
3      vals[], x[], y[]) {
4      #pragma omp parallel for
5      for i = 0 to num_ssr {
6          let ssr_start = ssr_ptr[i]
7          let ssr_end = ssr_ptr[i + 1]
8
9          for j = ssr_start to ssr_end {
10             let sr_start = sr_ptr[j]
11             let sr_end = sr_ptr[j + 1]
12
13             for k = sr_start to sr_end {
14                 let r_start = r_ptr[k]
15                 let r_end = r_ptr[k + 1]
16                 let temp = 0.0
17
18                 for l = r_start to r_end {
19                     temp += vals[l] * x[col_idx[l]]
20                 }
21                 y[k] = temp
22             }
23         }
24     }
25 }

```

ditional arrays that store data about rows (i.e., the number of additional arrays equals $k-1$). Figure 2 provides an example of CSR-3. In addition to the arrays for CSR, CSR-3 has two additional arrays. These arrays are `sr_ptr` and `ssr_ptr` that contain pointers to the super-rows and the super-super-rows. Super-rows are groups of contiguous rows, and the array is compressed in a similar manner to how `row_ptr` compresses information on the number of contiguous nonzeros in a row. Therefore, `sr_ptr=[1, 3, 6]` represents a sparse matrix with two super-rows: one spanning rows 1-2, and one spanning rows 3-5. This method is extended up to super-super-rows that group together contiguous super-rows. As a result, the CSR- k format's only memory overhead is the storage of these additional arrays. Moreover, applications and libraries that have not been fitted to utilize CSR- k , such as a visualization tools or checkpointing, can still process the format as they would a normal CSR format without the overhead of storing both. As such, this makes it an ideal base format for heterogeneous systems as most have support for CSR, even if not for CSR- k .

For completeness, we provide the pseudocode for SpMV with CSR-3 on a many-core system in Listing 1. Lines 4-5 parallelize the outermost `for` loop, which iterates over super-super rows (e.g., `num_ssr = 3` in Fig 2). In lines 6-9, the bounds for one super-super-row are fetched and iterated across (e.g., `ssr_ptr` in Fig 2). Similarly, lines 10-13 fetch the bounds for one super-row and are iterated across (e.g., `sr_ptr` in Fig 2). Finally, lines 14-21 implement the actual work in a similar manner to a CSR-based kernel.

CSR- k supports multiple reorderings. In particular, one for SpMV and one for sparse triangular solve as both require very different access patterns and have different structures (i.e., the ordering for SpMV tries to reduce access distance and the or-

dering for sparse triangular solve tires to minimize dependencies in the elimination graph). The ordering used by CSR- k for SpMV is called Band- k . This ordering applies band-reducing orderings (e.g., RCM) to the multiple levels the super-super-row and super-row structure provides. In order to apply these band reducing orderings, a graph representation of the rows (i.e., each row is a vertex and each nonzero is an edge) is generated. The vertices are coarsened into super-rows and super-super-rows, and the band reducing ordering is applied to each level of the coarsened row from the highest level (i.e., super-super-row for CSR-3) to the lowest level (i.e., row). This process normally produces an ordering with a band wider than that produced by RCM, but better fits the format structure. As such, we utilize the standard Band- k format for our extension as well. Moreover, the multiple levels of the coarsened-band ordering aims to try and help with load imbalance.

2.3. Formats for GPU

One notable format has a long history of being pushed on GPU, namely ELLPACK (ELL) format [16] and its derivatives. ELL format is a blocking format, which takes an $m \times n$ sparse matrix and stores it as two $m \times k$ dense matrices, where k is the number of nonzeros in the densest row of the sparse matrix. One matrix stores the nonzeros shifted left, padded on the right with zeros. The other matrix stores their corresponding columns also padded with zeros. ELL and its many variants were used heavily for GPU-based SpMV in the early days of GPGPU, due to its friendliness to vector architectures [20, 25], but suffer from the issue of excess memory overhead. For instance, if an irregular sparse matrix had the densest row containing 40 nonzeros, but an average nonzero count of 10, the ELL format would incur a 300% memory overhead. Due to the fact that GPUs often have much less memory than is allotted to the CPU, this means that many large irregular matrices that would fit with CSR format cannot fit using ELL format. Because of the potentially astronomical memory overhead incurred by ELL and its derivatives, we find ELL to be a failure on GPU.

2.4. Heterogeneous Formats

Heterogeneous formats are those that are designed to fit multiple different computational devices. These have become popular due to the importance of heterogeneous computing systems. Several popular formats stand out in this area. The first is the use of blocked sparse format on GPU devices. Eberhardt and Hoemmen [9] demonstrate that BCSR is a reasonable format for both many-core CPUs and GPUs when the sparse matrix contains some block substructure. However, a specialized algorithm for SpMV on GPU must be reworked for the particular device such as their *by-column* algorithm in order to out-compete NVIDIA’s built-in sparse matrix library cuSPARSE. On the other hand, Liu and Vinter [19]’s CSR5 introduces a CSR based format that utilizes a number of tiles to improve performance on both many-core CPUs and GPUs. These tiles are of size σ by ω and are autotuned to better fit the SIMD nature of the device. The elements in the `col_idx` are ordered in a way to fit these tiles and additional vectors (i.e., a title pointer

and a title descriptor with lengths that are based on the choice of σ and ω) are kept for title information along with a bit-flag the length of the number of nonzeros in the sparse matrix. Therefore, the format is tuned to the device, and storing the sparse matrix for additional devices would require keeping additional title pointers and title descriptors. Utilizing this format, CSR5 can obtain on average the maximum performance of either standard CSR or the autotuned pOSKI [1] on many-core CPU systems and is able to obtain on average the maximum performance of all tests kernels on GPUs. As such, the overheads for storing in CSR5 are somewhat similar to that of CSR- k , however, it is arguably a much more complex structure to understand and implement with so many tile level arrays, title pointer, title descriptors, and requiring bit-wise computations. Lastly, work by Aliaga et al. [3] examines the use of a compressed COO format. They demonstrate a truly heterogeneous format that can be stored in the same format for both many-core CPUs and GPUs. This format’s performance on CPU is on average better than Intel MKL’s CSR utilizing 16 AMD Epyc cores and is better on NVIDIA V100 and A100 than cuSPARSE’s COO. However, this format compresses values into integer values using a look-up table (LUT) and requires bit-wise computation for determining blocking. As such, both these methods are difficult for application scientists that may want to tune or modify an application.

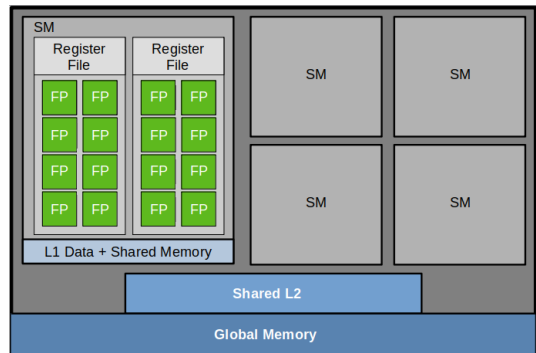


Figure 3: Diagram of the NVIDIA GPU memory hierarchy. A global shared memory (e.g., HBM2E) is at the bottom. A more standard L2 is shared by streaming multiprocessors (SM). Each SM has its own L1 that can act as a private data cache or shared memory. Each FP is a floating-point unit.

3. CSR- k for Exploiting Multidimensional Block Structure in NVIDIA GPUs

In this section, we provide an overview of how to extend CSR- k for NVIDIA GPUs utilizing CUDA. We note that there is nothing different in the storage format of CSR-3 for a GPU and the storage format of CSR-3 for a CPU that is introduced in the previous section. The difference is how we interpret the hierarchical levels within CSR- k and how this optimally gets implemented in the GPU algorithm. As noted before, the multiple levels in the CSR- k for a CPU can be interpreted as blocking sets of rows into super-super-rows and super-rows that better fit the hierarchical level cache structure on many-core systems. The algorithm implementation of this is straightforward with

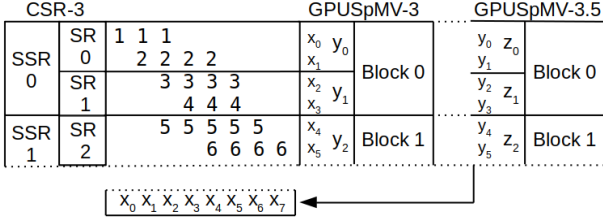


Figure 4: CUDA grid and block layout for GPU SpMV algorithms GPUSpMV-3 and GPUSpMV-3.5 in relationship to CSR-3.

each level providing an additional level of for-loops over the super-super-rows and super-rows. Listing 1 provides an example of this code for CSR-3 on a CPU.

However, NVIDIA GPUs utilizing CUDA do not have the same types of hierarchical level cache structure as a CPU. Figure 3 provides a representation of the memory and execution structure of a NVIDIA GPU. The GPU has a large (e.g., 80GB) shared global main memory consisting of HBM2 or HBM2E high-bandwidth memory for higher end systems, a shared L2 cache, and a memory layer that can be partitioned as a private L1 data cache or shared memory for each streaming multiprocessor (SM). We also note that these caches, such as the L1 data cache are much smaller per thread than a traditional CPU cache. For instance, AMD Rome (e.g., AMD Gen2 Epyc) has 32 KB per core of private L1 data cache, while the NVIDIA Ampere A100 has 192 KB per SM of L1 data cache. Since each SM has 64 32-bit floating-point units (FP), that equates to an average of 3 KB/thread, though this cache is shared across all FP execution units in an SM. Additionally, how these resources are scheduled are fundamentally different than a CPU. Each thread on a CPU can be fixed or pinned to a particular computational core and remain there until it has completed its work. In the CSR- k case, this work could be the execution of a particular set of super-rows. However, 32 threads are blocked together to form a warp on these GPUs. It is more convenient to think of this warp as a single SIMD intrinsic on CPUs. Groups of these threads/warps combine to form a thread block, and a thread block supports at most 1024 threads. These thread blocks are assigned to an SM and will not migrate to other SMs (i.e., they are fixed or pinned). Therefore, it is easier to think of each these blocks as an assignment of a core to a super-row. This mapping only goes so far as each SM may have multiple thread blocks and the order of execution of these thread blocks is unknown. These blocks are further coarsened into a grid. Due to how the scheduler is implemented, most efficient CUDA kernels are mapped into a computational grid or cube. This allows better exploitation of the 3D nature of CUDA blocks and the grid. Utilizing this structure often aids in better locality of data, since the CUDA runtime is able to schedule threads close in a block closer on the die. Using this cubic environment, we can map a multilevel data structure efficiently to a 2D or 3D block.

Therefore, we can utilize the hierarchical structure of the GPU even if not directly related to the cache level size for CSR- k , and in the next section we justify super-super-row and super-row sizes based on this argument if we utilize CSR-3 format. As

such, we will only focus on a $k = 3$ for these NVIDIA GPUs. We start by assuming that an SM is a core or shared-memory computational area in a standard CPU with a shared memory cache, i.e., the L1 data cache, even though each SM may have multiple blocks mapped to it and contains multiple dispatch units. This rationality is reasonable as a core may work on multiple super-super-rows and these super-super-rows should be issued as a chunk. Therefore, we can view a single block as a super-super-row each being assigned to an SM. As such, we build a grid of these blocks, i.e., a 1D grid. We note that a single block can only support up to 1024 threads, which will put a cap on the maximum size of our super-super-rows. Within a block, the next level (i.e., super-row) loop can be mapped to the y -dimension and the row can be mapped the x -dimension for form 2D blocks. We note that the order that x - and y -dimensions are structured in the code is important for GPU dispatch. Warps are grouped first by thread adjacency in the block x -dimension, then the y -dimension, then the z -dimension. Therefore, organizing the threads that work on the inner loops (which work on spatially adjacent data) along the x -dimension first is important for data locality. We call this base code GPUSpMV-3.

Figure 4 provides a diagram of the CSR-3 format’s layout in terms of CUDA thread blocks. As such, super-super-row 0 (SSR0) will map onto Block 0. The y -dimension of the block will be mapped on the the super-row (SR), e.g., y_0 maps to SR0 and y_1 maps to SR1. The accompanying pseudocode is provided in Listing 2. We note that this code is relatively simple and easy to implement in CUDA as it relies on the simple CSR-3 structure and CUDA block parallel functions.

The last for-loop, i.e., the inner product of the sparse matrix row and the vector, (Line 19-21 in Listing 2) in the algorithm provides an additional level of possible parallelism. The original CSR- k paper did not consider this level of parallelism because of overheads with aligning and data movement for SIMD intrinsics in the test hardware. As noted in the last section, CSR5 explicitly lays out its titles for these SIMD operations but at the cost of complexity of the format. This level of parallelism is important and needs to be addressed in GPU codes. However, if the number of nonzeros per row is relatively small (e.g., < 8), utilizing this level of parallelism would reduce the available number of overall threads to a block and would require the overhead of utilizing part of the L1 data cache for shared memory. Through experimentation, we discovered that 8 nonzero elements per row is what is require to improve perform with parallelization in this level. We denote the algorithm with the parallelism of the last level as GPUSpMV-3.5, and pseudocode is provided in Listing 3. Figure 3 also provides the structure for GPUSpMV-3.5. However, SSR are now the blocks, the SR are the z -dimension, the rows are the y -dimension, and nonzeros in the rows are the x -dimension.

For optimization purposes, we do a very aggressive loop unrolling for the innermost loop of GPUSpMV-3. The temp array in GPUSpMV-3.5 is allocated as a block-local shared memory space for fast read and write access.

Listing 2: GPUSpMV-3 GPU kernel

```

1  function cuSpMV_3(num_coarsest_rows, ssr_ptr[],
2                    sr_ptr[], r_ptr[], col_idx[],
3                    vals[], x[], y[]) {
4      let block = blockIdx.x
5      let ssr_start = ssr_ptr[block]
6      let sr_end = ssr_ptr[block + 1]
7
8      for i = ssr_start to ssr_end
9          parallelize across blockDim.y {
10             let sr_start = sr_ptr[i]
11             let sr_end = sr_ptr[i + 1]
12
13             for j = sr_start to sr_end
14                 parallelize across blockDim.x {
15                     let r_start = r_ptr[j]
16                     let r_end = r_ptr[j + 1]
17                     let temp = 0.0
18
19                     for k = r_start to r_end
20                         no parallelization {
21                             temp += vals[k] * x[col_idx[k]]
22                         }
23
24                     y[k] = temp
25                 }
26             }
27 }

```

Listing 3: GPUSpMV-3.5 GPU kernel

```

1  function cuSpMV_3.5(num_coarsest_rows, ssr_ptr[],
2                    sr_ptr[], r_ptr[], col_idx[],
3                    vals[], x[], y[]) {
4      let block = blockIdx.x
5      let ssr_start = ssr_ptr[block]
6      let ssr_end = ssr_ptr[block + 1]
7
8      for i = ssr_start to ssr_end
9          parallelize across blockDim.z {
10             let sr_start = sr_ptr[i]
11             let sr_end = sr_ptr[i + 1]
12
13             for j = sr_start to sr_end
14                 parallelize across blockDim.y {
15                     let r_start = r_ptr[j]
16                     let r_end = r_ptr[j + 1]
17                     let temp[blockDim.x] = fill(0.0)
18
19                     for k = r_start to r_end
20                         parallelize across blockDim.x {
21                             temp[threadIdx.x] +=
22                                 vals[k] * x[col_idx[k]]
23                         }
24                     y[k] = parallel_reduction(temp)
25                 }
26             }
27 }

```

3.1. Banding

The GPU algorithm still utilizes the banding of Band- k provided in [14]. While debate may exist on if ordering is important for GPU as it is with CPU, we find that it does. On GPU, banding can provide a significant advantage as opposed to a naturally ordered matrix. In Section 6, we provide evidence that ordering matters for GPU SpMV for CSR- k and one competitor SpMV library.

4. Tuning Optimal Structure

4.1. GPU

When tuning CSR- k for CPUs normally a low cost autotuning method is needed, and the original paper notes how inexpensive this autotuning is compared to pOSKI. Autotuning on a GPU opens up many new parameters, such as block dimensions and if the inner product should be parallelized (e.g., GPUSpMV-3 vs GPUSpMV-3.5). However, there exist some standards that can help guide this tuning, and these standards can even be reduced to a closed form heuristic formula that can determine the super-row and super-super-row sizes in constant time for a given sparse matrix after some initial tuning on a given device.

The first of these standards is based on the relationship between the number of threads and block size. Remember that only 1024 threads can be used per block and that 32 threads are launched at a time in a warp. Therefore, the dimensions of the block should be based off of multiples of 32. The second of these standard is having enough work to keep each thread busy, but limit the working memory size of each thread so accesses are not hitting slower caches or main memory. Additionally, making more threads is more likely to amortize any imbalance in work each thread might have. The average amount of work a single row must compute (in GPUSpMV-3) is based on the average row density, i.e., $rdensity = NNZ/N$ where NNZ is the number of nonzeros and N is the number of rows. Additionally, we have experimentally determined as noted before that serial computation of the inner product per row only makes sense when $rdensity < 8$. Based on these two facts and common block dimensions used in GPUs, we only need to consider the following cases:

Case 1: $rdensity \leq 8$

The block dimensions are set as 8×12 .

Case 2: $8 < rdensity \leq 16$

The block dimensions are set as $4 \times 8 \times 12$.

Case 3: $16 < rdensity \leq 32$

The block dimensions are set as $8 \times 8 \times 8$.

Case 4: $32 < rdensity \leq 64$

The block dimensions are set as $16 \times 8 \times 4$.

Case 5: $64 < rdensity$

The block dimensions are set as $32 \times 8 \times 2$.

We can interpret these values as follows. In Case 1, four rows along the y-dimension (i.e., 8×4 threads) would make up a

warp. Since the y -dimension corresponds to a super-row in GPUSpMV-3, a single warp would have four super-rows. This may seem like a lot of work, but the $rdensity$ is relatively small in this case. On the other hand, in Case 5, one row along the y -dimension would make up a warp due to the number of number of nonzeros in a single row needing to be computed.

Once these standard block sizes are set, empirical runs can be completed with different sizes of super-rows and super-super-rows over a suite of sparse matrices. We can use these runs with the following modeling method to determine a closed form heuristic for selection super-super-row and super-row sizes in the future. Using these test runs, we perform a logarithmic regression over the dataset, with the x -values being $rdensity$ and the y values being the optimal super-super-row or super-row sizes. The $SSRS$ (super-super-row size) and SRS (super-row size) parameters are tuned independently. That is, during testing, all reasonable combinations of $SSRS$ and SRS are tested (some set of representative sizes between 4 and 48 for GPU) and the regression is performed twice: one on the optimal $SSRS$ parameters, and one on the optimal SRS parameters. The specific set of combinations for $SSRS$ and SRS tested are described as follows:

$$(SSRS, SRS) \in \left(\bigcup_{i=2}^5 \{2^i, 1.5 \cdot 2^i\} \right)^2$$

where ϕ^2 is shorthand for the set Cartesian product $\phi \times \phi$.

Finally, since the logarithmic distribution tends to yield a formula that drops much below optimal when $rdensity$ becomes large, the coefficient of the natural logarithm was lowered by hand to better fit the optimal $SSRS$ and SRS with high $rdensity$.

From this method, we achieve the following formula for tuning on the NVIDIA Volta V100:

$$SSRS = \lfloor 8.900 - 1.25 \cdot \ln(rdensity) \rfloor$$

and

$$SRS = \lfloor 10.146 - 1.50 \cdot \ln(rdensity) \rfloor.$$

where $\lfloor x \rfloor$ represents a round-to-nearest, half towards positive infinity operation.

These numbers would have to be derived for each different machine that has considerable microarchitecture differences. For NVIDIA Ampere, a slight tuning is required. The same process is used:

$$SSRS = \lfloor 9.175 - 1.32 \cdot \ln(rdensity) \rfloor$$

and

$$SRS = \lfloor 20.500 - 3.50 \cdot \ln(rdensity) \rfloor.$$

As with Ampere, the coefficient of the natural logarithm is lowered so that the $SSRS$ and SRS do not drop too low on the higher row densities. The constant term is unchanged in both instances.

After the initial $SSRS$ and SRS are determined, they can be further tuned based on $rdensity$. In particular, the $SSRS$ and SRS need to be updated to account from their derivation from

the original assumption of utilizing GPUSpMV-3 to GPUSpMV-3.5, in addition to accounting for the changing block dimensions as $rdensity$ grows. As such, they are modified as follows on NVIDIA Volta:

Case 1: $rdensity \leq 8$

Tune SSRS and SRS no further.

Case 2: $8 < rdensity \leq 16$

$$SSRS = \lfloor SSRS \times 1.5 \rfloor$$

$$SRS = SRS \times 2.$$

Case 3: $16 < rdensity \leq 32$

$$SSRS = SSRS \times 4$$

$$SRS = \lfloor SSRS/2 \rfloor.$$

Case 4: $32 < rdensity$

$$SSRS = SSRS \times 5$$

$$SRS = \lfloor SSRS/2 \rfloor.$$

And as follows on NVIDIA Ampere:

Case 1: $rdensity \leq 8$

Tune SSRS and SRS no further.

Case 2: $8 < rdensity \leq 16$

Tune $SSRS$ no further.

$$SRS = SRS \times 4.$$

Case 3: $16 < rdensity \leq 32$

$$SSRS = \lfloor SSRS \times 2.5 \rfloor$$

$$SRS = SSRS \times 3.$$

Case 4: $32 < rdensity \leq 64$

$$SSRS = SSRS \times 2$$

$$SRS = SSRS \times 2.$$

Case 5: $64 < rdensity$

$$SSRS = \lfloor SSRS \times 2.7 \rfloor$$

$$SRS = \lfloor SSRS/4 \rfloor.$$

4.2. CPU

On CPU, CSR-2 is used following the findings of [14]. When running CSR-2 on a CPU, the kernel is much less dependent on having optimal $SSRS$ and SRS within a narrow window for good performance. Additionally, the added complexity of the cache hierarchy in CPUs as opposed to GPUs makes tuning much more difficult to do optimally, as there is no clear correlation between optimal $SSRS/SRS$ and known matrix attributes without analyzing matrix structure. Due to these combinations of factors, we find that in an ideal scenario, each matrix would be tuned individually, using a set of representative SRS between 8 and 3072, which are specified as the set:

$$SRS \in \bigcup_{i=3}^{11} \{2^i, 1.5 \cdot 2^i\}$$

The combined effect of larger caches on CPU and using CSR-2 instead of CSR-3 means that much higher SRS are often preferred. Namely, most matrices on CPU using CSR-2 prefer

SRS in the range of 40-1000, as opposed to most matrices on GPU using CSR-3 preferring $SSRS/SRS$ in the range of 4-12.

If constant-time tuning is preferred at the expense of performance, we have found that taking the geometric mean of optimal SRS across a representative dataset yields decent performance. For instance, one might use a $SRS = 96$ for all matrices on CPU to yield performance that is often “good enough.” This is explored empirically in Section 7.

5. Test Setup

5.1. Test Systems

The test setup consists of four systems. System 1 is used for GPU testing and has two Xeon E5-2650v4 CPUs (“Broadwell”) with 12 cores each, and contains several NVIDIA V100 GPUs (“Volta”). These GPUs contain 32 GB of main memory, and peak memory bandwidth of 900 GB/s. System 2 is also used for GPU testing and has two Epyc 7713 CPUs (“Milan” or “Zen 3”) with 64 cores each, and contains NVIDIA A100 GPUs (“Ampere”). These GPUs contain 40 GB of memory, and a peak memory bandwidth of 1555 GB/s. On both GPU systems, only one GPU is used. System 3 is for CPU testing. It contains two Epyc 7742 CPUs (“Rome” or “Zen 2”) and 256 GB of memory in 8 memory channels. Simultaneous multi-threading (SMT) is disabled for system 3. System 4 is also for CPU testing, and contains two Intel Xeon Platinum 8380 CPUs (“Ice Lake Server”) and 256 GB of memory. SMT is enabled for system 4, but we opt not to use it in tests. Table 1 provides details on each of these systems.

5.2. Tested Libraries

For GPU experiments, GPUSpMV-3 and GPUSpMV-3.5 are both implemented in C++ with CUDA and compiled with the NVIDIA’s NVHPC compiler using compilation tools version 11.4. Our CSR- k SpMV implementations are compared against cuSPARSE v11.4 and KokkosKernels v3.4.1 [10]. NVIDIA’s cuSPARSE is an optimized sparse linear algebra library written for use on NVIDIA GPUs. It provides SpMV implementations in a number of formats, and we compare against the library’s CSR implementation. NVIDIA’s cuSPARSE is part of the CUDA runtime, so all runs are performed using CUDA runtime 11.4, which has support for both Volta and Ampere GPUs. KokkosKernels is a computational mathematics library published by Sandia National Laboratories. It supports sparse and dense linear algebra, among other kernels, on both CPUs and GPUs. The goal of KokkosKernels is to provide performance portable code to a number of parallel runtime libraries without requiring the user to code in the different libraries. KokkosKernels is compiled for the SM_70 compute architecture, which is supported by our Volta GPUs. The tested version of KokkosKernels does not support a build parameter for SM_80, i.e., the compute architecture used by newer Ampere GPUs, and therefore will only be tested on Volta.

For CPU experiments, we utilize Intel MKL v19.1.3 on system 3 and Intel MKL v19.1.1 on system 4. Intel MKL (Math

Kernel Library) is a computational mathematics library that supports highly-optimized sparse linear algebra on CPUs. CSR- k is compiled on system 3 with the AMD Optimizing C Compiler (AOCC) v2.3.0 with `-O3` optimization and `-march=znver2`. CSR- k is compiled on system 4 with the Intel v19.1.1 compiler with `-O3 -ipo` optimization and `-march=icelake-server`. On both system 3 and system 4, compiler pragmas are used to enable the maximum vectorization width for the innermost loop (8-way SIMD on system 3 and 16-way SIMD on system 4) for CSR- k . Additionally, OpenMP scheduling parameters are set to `schedule(static)` for CSR- k on systems 3 and 4.

5.3. Test Suite

We use 16 representative sparse matrices from the SuiteSparse matrix collection [8]. Table 2 provides a list of all sparse matrices along with their outermost dimension (N), number of nonzeros (NNZ), and row density ($rdensity$). Sparse matrices are listed in order of increasing $rdensity$. These sparse matrices range from N as small as 62,631 (brack2) to as large as 18,318,143 (hugebubbles-00000) and $rdensity$ from as sparse as 2.758 (roadNet-TX) to as dense as 71.53 (bmwcr1).

For KokkosKernels, cuSPARSE, and MKL, all sparse matrices are first reordered utilizing RCM obtained from GNU Octave’s `symrcm`. As noted before, RCM provides improve converge for some iterative solvers (e.g., CG) and improves performance due to reducing the stride of irregular accesses. We opt to feed CSR- k with matrices in their natural ordering to demonstrate the efficacy of the Band- k algorithm [2]. This will demonstrate even when competing algorithms are fed with bandwidth-reducing reorderings, Band- k and CSR- k are able to match and outperform existing highly-optimized implementations of SpMV.

5.4. Test Methodology

For GPU tests, data is copied ahead of time to the GPU, and only the SpMV kernel execution time is measured. This is done to accurately model the behavior of iterative solvers, which should not re-copy the data each iteration. For both CPU and GPU tests, 20 runs are performed and the results are averaged via arithmetic mean. On CPU tests, 5 untimed warmup runs are performed, because MKL appears to take 1-2 iterations before reaching maximum performance. For instance, when the matrix hugebubbles in RCM ordering is run 20 times under MKL without a warmup, the first iteration takes $\sim 2.8\times$ longer than subsequent iterations. CSR- k is given the same 5 warmup runs for fairness.

cuSPARSE appears to show the same behavior, but only for poorly or badly reordered matrices. For example, the same hugebubbles matrix in its natural ordering takes $\sim 37\times$ longer the first iteration than subsequent iterations, but its RCM ordering only takes $\sim 1.5\times$ longer the first time than subsequent runs. Since we are giving cuSPARSE RCM-ordered matrices, we opt to not perform any warmup runs on GPU. KokkosKernels does not appear to display any similar behavior.

Table 1: All systems we use for testing.

System	Label	CPU	Physical Cores	Memory	GPU	GPU Memory
1	Volta	Intel Xeon E5-2650v4	24	128 GB	NVIDIA V100	32 GB
2	Ampere	AMD Epyc 7713	128	1 TB	NVIDIA A100	40 GB
3	Rome	AMD Epyc 7742	128	256 GB	None	None
4	Ice Lake	Intel Xeon Platinum 8380	80	256 GB	None	None

Table 2: Test suite of matrices including their name, (N), number of nonzeros (NNZ), and row densities (*rdensity*).

ID	Matrix	N	NNZ	<i>rdensity</i>	Problem Type
1	roadNet-TX	1,393,383	3,843,320	2.76	Undirected Graph
2	hugetrace-00000	4,588,484	13,758,266	2.99	DIMACS
3	hugetric-00000	5,824,554	17,467,046	2.99	DIMACS
4	hugebubbles-00000	18,318,143	54,940,162	2.99	DIMACS
5	wi2010	253,096	1,209,404	4.77	DIMACS
6	G3_circuit	1,585,478	7,660,826	4.83	Circuit Simulation
7	fl2010	484,481	2,346,294	4.84	DIMACS
8	ecology1	1,000,000	4,996,000	4.99	2D/3D Problem
9	cont-300	180,895	988,195	5.46	Optimization Problem
10	delaunay_n20	1,048,576	6,291,372	6.00	DIMACS
11	thermal2	1,228,045	8,580,313	6.98	Thermal Problem
12	brack2	62,631	733,118	11.71	2D/3D Problem
13	wave	156,317	2,118,662	13.55	2D/3D Problem
14	packing-500x100x100	2,145,852	34,976,486	16.30	DIMACS
15	Emilia_923	923,136	40,373,538	43.74	Structural Problem
16	bmwcra_1	148,770	10,641,602	71.53	Structural Problem

6. GPU Performance

In this section, we analyze the performance of CSR-3 on Volta and Ampere GPUs. We tune the super-super-row and the super-row sizes based on the automatic analysis base tuning in Section 4. We compare these results to both the CSR representation format in cuSPARSE and KokkosKernels for the Volta and only cuSPARSE on the Ampere due to KokkosKernels’s current compiler limitations. We utilize two forms of measurement for performance. The first measures GFlop/s which is the standard method in other works [3, 19] related to SpMV on GPUs to provide raw performance numbers. The second measure is relative performance compare to cuSPARSE defined as:

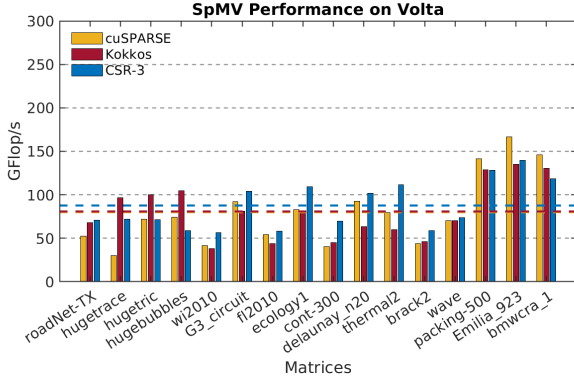
$$\text{Relative Perform}(m) = \frac{\text{time}(cuSPARSE, m) - \text{time}(CSR-3, m)}{\max(\text{time}(cuSPARSE, m), \text{time}(CSR-3, m))} \times 100$$

where m is the given sparse matrix.

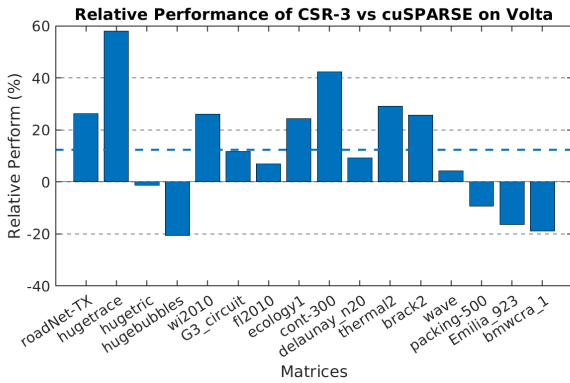
Relative performance is one of the main performance metrics we use in this paper. We choose this metric because scaling is mirrored across 0. In essence, if CSR-3 is twice as fast as cuSPARSE, this metric will show 50% relative performance. If CSR-3 is half as fast as cuSPARSE, this metric will show -50% relative performance. This metric is not a linear scaling, but rather a reciprocal scaling. So, if CSR-3 is three times as fast as cuSPARSE, this metric will show 67% relative performance, and if CSR-3 is four times as fast, this metric will show 75% relative performance. Assuming some fixed cuSPARSE

time, as the time to compute a CSR-3 kernel approaches 0, this metric will approach 100%, and as the time to compute CSR-3 approaches ∞ , this metric will approach -100%. Finally, this metric shows 0% if CSR-3 and cuSPARSE are equally as fast.

Figure 5 provides the performance observations for Volta. The top figure (i.e., 5a), provides the GFlop/s as bars, and the dashed lines are the average GFlop/s for the test suite. The average GFlop/s for this test suit is 79.6 GFlop/s for cuSPARSE, 80.9 GFlop/s for KokkosKernels, and 87.7 GFlop/s for CSR-3. We note that the matrices are ordered based on their *rdensity* from left to right. In theory, the more dense sparse matrices increase the potential computational intensity and should achieve a higher GFlop/s. We do observe this trend with the last three matrices performing over 100 GFlop/s. Overall CSR-3 does outperform the other two formats except in a couple of cases. These two cases are the matrices generated from graphs in the DIMAC challenge (i.e., matrices 2-4) and the matrices with higher *rdensity* (i.e., matrices 14-16). In the first case, KokkosKernels is the best. We believe that this is due to KokkosKernels being highly tuned for this set of matrices as observed by numerous publications from the KokkosKernels group on DIMAC. As for the more dense matrices, CSR-3 is outperformed by cuSPARSE even with CSR-3 utilizing our GPU-SpMV-3.5 method. However, we note that most sparse matrices from partial differential equations (PDEs) that would utilize an iterative solve method (e.g., CG and GMRES) have *rdensity* < 40. In the lower figure, the relative performance is reported. The average relative performance improvement is



(a) GFlop/s on Volta



(b) Relative perform on Volta

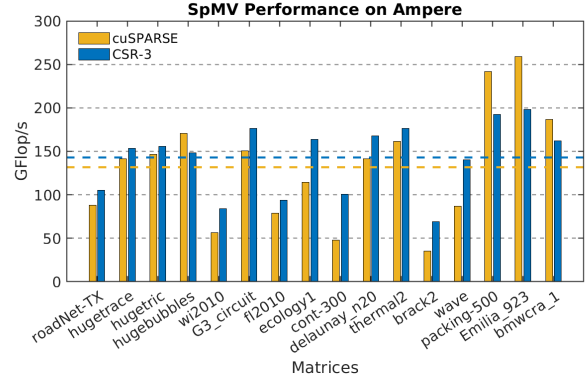
Figure 5: Performance on Volta. With a couple exceptions, CSR- k tends to outperform cuSPARSE and KokkosKernels with higher relative perform and GFlop/s.

17.3% over cuSPARSE.

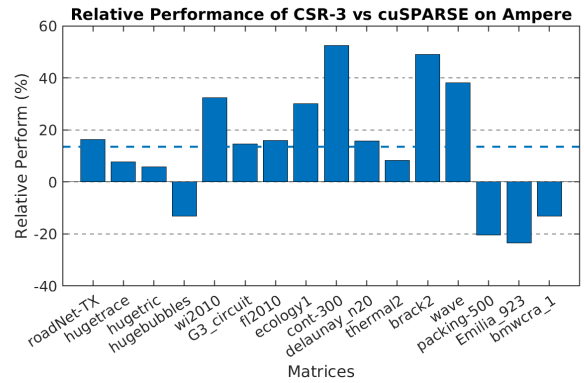
Figure 6 provides the performance on Ampere. The Ampere card is a big improvement relative to Volta. Ampere has a maximum peak 32-bit floating-point performance of 19.5 teraflop/s compared to the 15.7 teraflop/s of the Volta card. However, the major difference comes in the form of the memory hierarchy. The main memory of Ampere is much larger, the L2 cache is 7 \times larger, and a new asynchronous copy directly from global memory to shared memory has been introduced. The top figure (i.e., 6a) provides the GFlops/s for the test suite on Ampere when autotuning parameters for Ampere are found. We observe the average GFlop/s for cuSPARSE is 131.72 GFlop/s and for CSR-3 is 142.93 GFlop/s. Again, CSR-3 outperforms cuSPARSE on almost all sparse matrices except the last three very dense ones. The bottom figure (i.e., Figure 6b) provides the relative performance, and we observe the average relative performance increase of approximately 18.9%.

6.1. Banding

We also perform a banding evaluation to ensure that the performance increase from CSR- k is not due to a superior banding algorithm. We assert that the used implementation of Band- k is rather poor when compared to RCM, and thus puts CSR- k at a *disadvantage*.



(a) GFlop/s on Ampere



(b) Relative perform on Ampere

Figure 6: Performance on Ampere. As with Volta, CSR- k tends to outperform cuSPARSE with a couple exceptions.

To demonstrate this assertion, we test KokkosKernels with matrices in their natural ordering, Band- k reordered matrices reduced to CSR, and RCM ordering. Additionally, we test CSR- k with Band- k matrices, and with RCM matrices that are then fed into Band- k for a second reordering. We do not test MKL or cuSPARSE as it is unknown from documentation and observations of warmup cost (Section 5.4) if either of these does any reordering of their own. This last test is to simulate the potential performance gains from a more intelligent Band- k implementation. For comparison, we take the arithmetic mean of relative performance compared to KokkosKernels with RCM ordering. Thus, the KokkosKernels (RCM) bar will show as 0 on the graph, with less performant configurations < 0 and more performant configurations > 0 .

Results are shown in figure 7. All CSR- k configurations have a positive relative performance, demonstrating that they are outperforming KokkosKernels with RCM ordering. KokkosKernels with Band- k ordering is the worst performing in the suite, underperforming even KokkosKernels with no ordering whatsoever. Thus, we may conclude that the performance gains are not due to a superior banding algorithm and that in fact, CSR- k leaves performance on the table with a sub-par banding implementation.

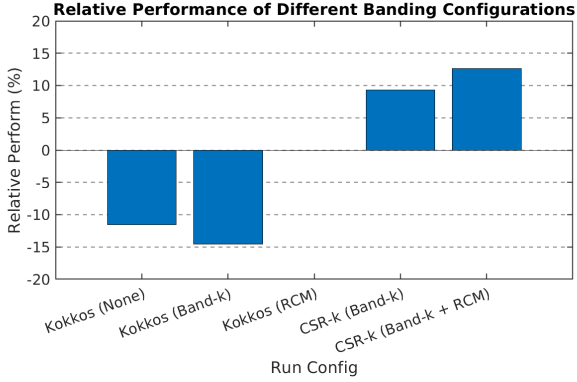


Figure 7: Banding analysis of KokkosKernels and CSR- k with miscellaneous banding combinations. Band- k ordering performs worse than RCM or natural ordering when using Kokkos.

7. CPU Performance

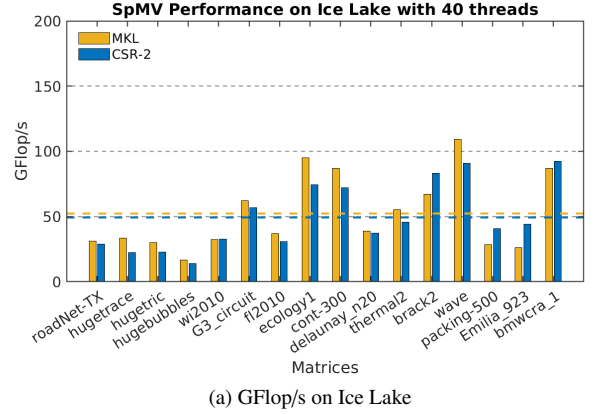
In this section, we verify the ability of CSR- k to improve performance on CPUs. This is necessary as the original paper was printed over eight years ago (2014), and the design of CPUs has changed. In particular, the three design changes have been increased core count on a single socket, different caching structures (e.g., multiple segmented shared caches as in Rome), and different hardware reuse techniques (e.g., newer Intel systems).

In order to keep the same style as the previous section, we report the GFlop/s for a thread count matching the core count on one socket (e.g. 64 threads on Rome and 40 threads on Ice Lake). We further provide a scalability study for a handful of representative thread counts. Finally, we demonstrate the performance penalty incurred by a constant-time tuning via fixed super-row size. We utilize CSR-2 for these experiments and test against Intel Math Kernel Library. The average GFlop/s is reported as a dashed line in figures 8a and 9a. For these average cases, we notice that CSR- k is usually on-par with MKL, falling slightly behind in GFlop/s. On Ice Lake, MKL had an average of 52.3 GFlop/s, while CSR- k had an average of 49.3 GFlop/s. On Rome, the numbers are even closer, where MKL had an average of 75.1 GFlop/s and CSR- k had an average of 72.5 GFlop/s. We use the same relative performance metric from the GPU section, defined here as

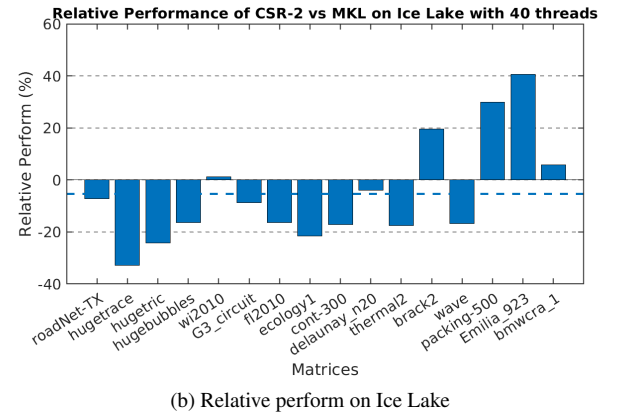
$$\text{Relative Perform}(m) = \frac{\text{time}(\text{MKL}, m) - \text{time}(\text{CSR-3}, m)}{\max(\text{time}(\text{MKL}, m), \text{time}(\text{CSR-3}, m))} \times 100$$

where m is the given sparse matrix. Figures 8b and 9b provide the relative performance of CSR- k versus MKL. We notice on Ice Lake that CSR- k is about -5.4% relative performance compared to MKL, while on Rome, CSR- k is about 1.3% relative performance compared to MKL.

Figures 10a and 10b presents our scalability study. For Ice Lake, we choose the core counts $c \in \{1, 4, 16, 40\}$, and on Rome we choose $c \in \{1, 4, 16, 64\}$. Results are the geometric mean of speedup across all matrices, and results are normalized to MKL on 1 core for both systems. We notice that on Ice Lake,



(a) GFlop/s on Ice Lake



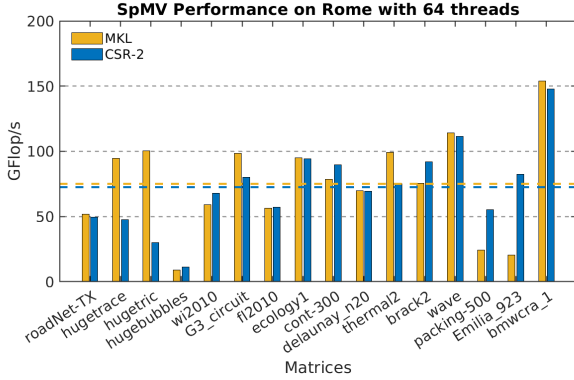
(b) Relative perform on Ice Lake

Figure 8: Performance on Ice Lake. MKL tends to perform better, but not by a huge margin.

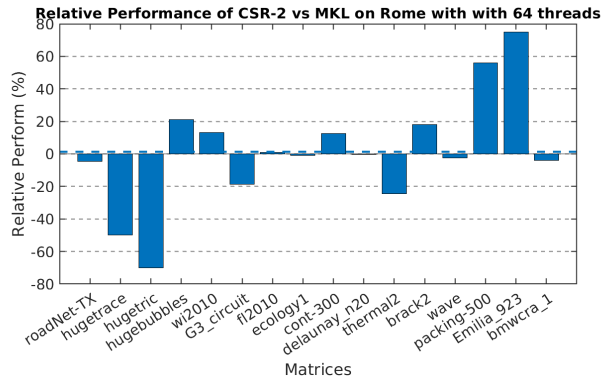
MKL tends to outperform CSR-2 on all core counts. However, both algorithms scale very well, with a maximum speedup of $\sim 28.5\times$ on 40 cores for MKL, and $\sim 25.5\times$ on 40 cores for CSR-2. On Rome, MKL scales better up to 4 cores, where it is then surpassed by a thin margin by CSR-2 for higher core counts. On 64 cores, MKL achieves a maximum speedup of $\sim 31.7\times$, and CSR-2 achieves its maximum of $\sim 32.7\times$.

Compared to the GPU implementation of CSR-3, the CPU implementation of CSR-2 is relatively unoptimized and naive. We use simple OpenMP statically-scheduled parallelism on the outermost loop and compiler-specific vectorization pragmas on the innermost loop. Finally, on Rome, we found that prefetching some values via compiler intrinsics can help for larger matrices with $NNZ > 12,500,000$. However, we do not consider the CPU implementation to be particularly optimized when compared to the GPU implementation. We suspect that more aggressive optimizations could be beneficial in closing the performance gap on both CPU systems. Several routes for optimization were explored, such as unrolling-and-jamming the innermost 2 loops [5], aggressive AVX intrinsics, and a miscellany of compiler-specific pragmas. However, we have not extensively exhausted all possible routes for optimization, and leave this as a future avenue of exploration.

Figure 11 shows the results of our best attempt at a constant-time tuning for CPU-based CSR- k . We take the geometric mean



(a) GFlop/s on Rome

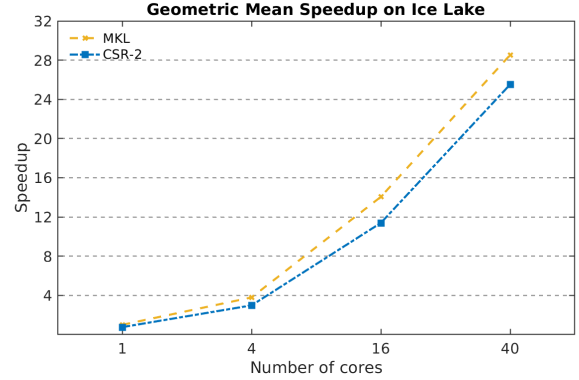


(b) Relative perform on Rome

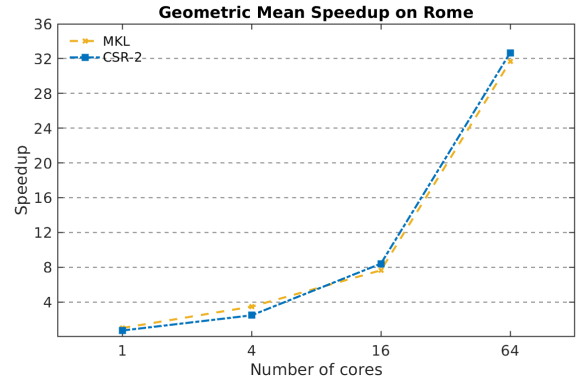
Figure 9: Performance on Rome. MKL and CSR- k perform roughly identically.

of optimal super-row sizes across the dataset, which is 81. We round this up to 96, which was in our super-row test set as mentioned in section 4.2. Finally, all matrices are tested with a fixed super-row size of 96. The relative performance metric is used once again. The majority of the matrices perform very well, with about -5% relative performance or better compared to their optimal tunings. However, there are a handful of outliers like hugebubbles or Emilia_923 which are much more sensitive to an optimal super-row size. Many of these matrices prefer a super-row size in a very narrow window and are largely agnostic to changes outside that window. We are unsure what causes this. Overall, we note that with the outliers in the dataset, using a fixed $SRS = 96$ results in a performance hit of -10.2% relative performance. With the four most significant outliers removed from the dataset (those with relative performance $< -20\%$), the performance hit is -3.5% relative performance.

Finally, we note that the optimal super-row size can vary greatly, but usually doesn't significantly impact performance, aside from some outliers. Consistent with the findings in [14], usually a super-row size between 40 and 1000 works well. However, there were several matrices that preferred very small super-row sizes (such as brack2 which performed optimally with a SRS of 8), and one that preferred a very large super-row size (hugebubbles which performed optimally with a SRS of 2048).



(a) Scalability on Ice Lake



(b) Scalability on Rome

Figure 10: Scalability study. CSR- k is able to scale nearly equally to MKL on Rome, though less than optimally on Ice Lake.

8. Analysis

We lastly want to analyze the cost of utilizing CSR- k as a heterogeneous format. There are two costs to consider, namely: step up cost and memory overhead for storage. For the former, we argue that the original work and add-on triangular solution work demonstrates that the setup cost could be amortized over the multiple uses in the application. Moreover, these works demonstrate that CSR- k 's setup cost is lower than an autotuning method such as pOSKI. Our additional use of a formula-driven autotuning for GPUs in Section 4 reduces the cost of tuning a particular sparse matrix for a GPU once autotuning derives the parameters of the formula. For a test suite of our size, this autotuning to derive the needed parameters can be done in under four hours. Therefore, we claim that the tuning time is more than acceptable since you only need to derive the parameters once for a new device and additional sparse matrices can be tuned using the derived formula in constant time.

The second measure to consider is overhead and is one of the advantages of CSR- k . Figure 12 provides the overhead percentage of utilizing just CSR-3 for GPU processing and CSR-3 + CSR-2 for GPU and CPU processing over CSR. In this diagram for CSR-3, we use the $SSRS$ and SRS determined by the closed-form heuristic explored in section 4. For CSR-2, we use an $SRS = 96$, as this is close to the geometric mean of optimal SRS across the dataset, also mentioned in section 4.

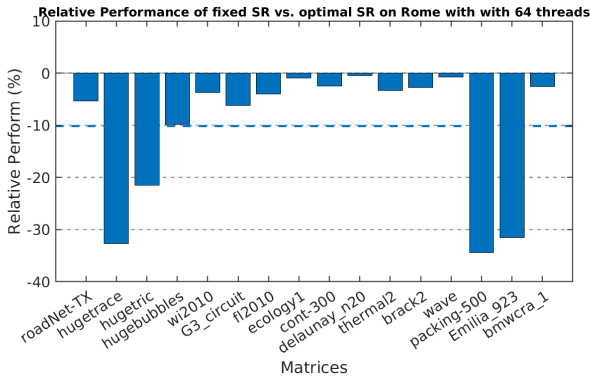


Figure 11: Constant super-row size on Rome, with SR fixed to 96. Most matrices tend to perform only slightly less optimally, with a few outliers being very sensitive.

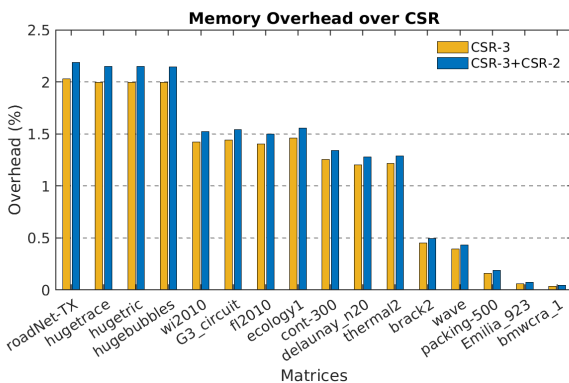


Figure 12: Storage overhead percentage of CSR-3 versus base CSR.

We observe that the cost of keeping both CSR-3 and CSR-2 data only requires a couple of additional arrays of super-row pointers and does not add much to the overhead. In the worst case (i.e., roadNet-TX), the overhead is just slightly over 2% for the combined format. We also notice a trend that as the *rdensity* becomes very large, the overhead decreases. Two factors contribute to this trend. The first factor is that the Band- k ordering will more aggressively combine nodes in the coarsen phase due to the number of heavy edges. The second factor is due to our tuning and utilization of GPUSpMV-3.5. In the tuning of GPUSpMV-3.5, we try to exploit as many SIMD operations in a single row by adding a new dimension. However, since the max number of threads is fixed in a block (i.e., 1024), the number of threads that can be assigned to the outer dimension decreases and so these blocks are normally made larger. The final factor is that the `vals` and `col_idx` matrix take up proportionally more space when compared to the compressed row pointers as row density increases.

The low storage overhead for CSR- k is important in two ways. First, it demonstrates that CSR- k should not put excess demand on the memory subsystem compared to CSR, which is important for sparse matrix formats since SpMV is limited by memory bandwidth. Second, it demonstrates that a matrix in CSR- k format should run on most or all devices that are capable of running the same matrix in CSR format. This is a testament

to the portability and heterogeneity of the format, as a matrix in CSR- k format has sufficiently small overhead to conceivably run on the vast majority of computational devices that can run equivalent CSR matrices.

9. Conclusion

An efficient heterogeneous format for SpMV is required by modern high-performance computing. This format needs to be easy to understand, easy to tune, and provide portable performance across devices without using too much additional memory overhead or time to tune. This paper presents CSR- k as a heterogeneous format solution for SpMV. This CSR based format is easy to understand, can be tuned quickly, and can be used as-is by library calls that require a standard CSR format. Mover, we present a method to tune CSR-3 in constant time for a particular sparse matrix utilizing an autotuned formula model. Using tuned CSR- k , the format method outperforms NVIDIA’s cuSPARSE by $\sim 17.3\%$ on Volta and $\sim 18.9\%$ on Ampere GPUs. On AMD Rome and Intel Ice Lake CPUs, CSR- k maintains comparable performance to Intel MKL, though falls slightly behind on Ice Lake. We suspect further hand-tuning of the implementation could close this gap. Moreover, the additional memory overhead to keep this heterogeneous format for both GPU and CPU devices was $< 2.5\%$ over standard CSR. Therefore, we demonstrated that CSR- k is an ideal heterogeneous format for many-core CPUs and NVIDIA GPUs.

Acknowledgement

This work was made possible in part by support from the Alabama Supercomputer Authority, Sandia National Laboratories, and NSF2044633. This work used the Extreme Science and Engineering Discovery Environment (XSEDE), which is supported by National Science Foundation grant number ACI-1548562.

References

- [1] pOSKI: Parallel optimized sparse kernel interface. URL <https://bebop.cs.berkeley.edu/poski/>.
- [2] The effect of ordering on preconditioned conjugate gradients. *BIT Numerical Mathematics*, 29:635–657, 1989.
- [3] José I. Aliaga, Hartwig Anzt, Thomas Grützmacher, Enrique S. Quintana-Ortí, and Andrés E. Tomás. Compression and load balancing for efficient sparse matrix-vector product on multicore processors and graphics processing units. *Concurrency and Computation: Practice and Experience*, page e6515. doi: <https://doi.org/10.1002/cpe.6515>.
- [4] Stephen T. Barnard, Alex Pothén, and Horst Simon. A spectral algorithm for envelope reduction of sparse matrices. *Numerical Linear Algebra with Applications*, 2(4):317–334, 1995.
- [5] S. Carr, Chen Ding, and P. Sweany. Improving software pipelining with unroll-and-jam. In *Proceedings of HICSS-29: 29th Hawaii International Conference on System Sciences*, volume 1, pages 183–192 vol.1, 1996. doi: 10.1109/HICSS.1996.495462.
- [6] Shizhao Chen, Jianbin Fang, Donglin Chen, Chuanfu Xu, and Zheng Wang. Adaptive optimization of sparse matrix-vector multiplication on emerging many-core architectures. In *2018 IEEE 20th International Conference on High Performance Computing and Communications; IEEE 16th International Conference on Smart City; IEEE 4th International Conference on Data Science and Systems (HPCC/SmartCity/DSS)*, pages 649–658, 2018. doi: 10.1109/HPCC/SmartCity/DSS.2018.00116.

- [7] E. Cuthill and J. McKee. Reducing the bandwidth of sparse symmetric matrices. In *Proceedings of the 1969 24th National Conference*, ACM '69, page 157–172, New York, NY, USA, 1969. Association for Computing Machinery. ISBN 9781450374934. doi: 10.1145/800195.805928.
- [8] Timothy A. Davis and Yifan Hu. The university of florida sparse matrix collection. *ACM Trans. Math. Softw.*, 38(1), dec 2011. ISSN 0098-3500. doi: 10.1145/2049662.2049663.
- [9] Ryan Eberhardt and Mark Hoemmen. Optimization of block sparse matrix-vector multiplication on shared-memory parallel architectures. In *2016 IEEE International Parallel and Distributed Processing Symposium Workshops (IPDPSW)*, pages 663–672, 2016.
- [10] H. Carter Edwards and Christian R. Trott. Kokkos: Enabling performance portability across manycore architectures. In *2013 Extreme Scaling Workshop (xsw 2013)*, pages 18–24, 2013. doi: 10.1109/XSW.2013.7.
- [11] István R eguly and Mike Giles. Efficient sparse matrix-vector multiplication on cache-based gpus. In *2012 Innovative Parallel Computing (InPar)*, pages 1–12, 2012. doi: 10.1109/InPar.2012.6339602.
- [12] Alan George and Joseph W. Liu. *Computer Solution of Large Sparse Positive Definite*. Prentice Hall Professional Technical Reference, 1981. ISBN 0131652745.
- [13] Michael A. Heroux, Padma Raghavan, and Horst D. Simon. *Parallel Processing for Scientific Computing*. Society for Industrial and Applied Mathematics, 2006. doi: 10.1137/1.9780898718133.
- [14] Humayun Kabir, Joshua Dennis Booth, and Padma Raghavan. A multilevel compressed sparse row format for efficient sparse computations on multicore processors. In *2014 21st International Conference on High Performance Computing (HiPC)*, pages 1–10, 2014. doi: 10.1109/HiPC.2014.7116882.
- [15] Humayun Kabir, Joshua Dennis Booth, Guillaume Aupy, Anne Benoit, Yves Robert, and Padma Raghavan. STS-k: A multilevel sparse triangular solution scheme for numa multicores. In *Proceedings of the International Conference for High Performance Computing, Networking, Storage and Analysis, SC '15*, New York, NY, USA, 2015. Association for Computing Machinery. ISBN 9781450337236. doi: 10.1145/2807591.2807667. URL <https://doi.org/10.1145/2807591.2807667>.
- [16] David Kincaid, Thomas Oppe, and David Young. Itpackv 2d user's guide. URL <https://web.ma.utexas.edu/CNA/ITPACK/manuals/userv2d/>.
- [17] Orhan Kislal, Wei Ding, Mahmut Kandemir, and Ilteris Demirkiran. Optimizing sparse matrix vector multiplication on emerging multicores. In *2013 IEEE 6th International Workshop on Multi-/Many-core Computing Systems (MuCoCoS)*, pages 1–10, 2013. doi: 10.1109/MuCoCoS.2013.6633600.
- [18] JaeHyuk Kwack, John Tramm, Colleen Bertoni, Yasaman Ghadar, Brian Homerding, Esteban Rangel, Christopher Knight, and Scott Parker. Evaluation of performance portability of applications and mini-apps across amd, intel and nvidia gpus. In *2021 International Workshop on Performance, Portability and Productivity in HPC (P3HPC)*, pages 45–56, 2021. doi: 10.1109/P3HPC54578.2021.00008.
- [19] Weifeng Liu and Brian Vinter. CSR5: An efficient storage format for cross-platform sparse matrix-vector multiplication. In *Proceedings of the 29th ACM on International Conference on Supercomputing, ICS '15*, page 339–350, New York, NY, USA, 2015. Association for Computing Machinery. ISBN 9781450335591. doi: 10.1145/2751205.2751209.
- [20] Marco Maggioni and Tanya Berger-Wolf. Adell: An adaptive warp-balancing ell format for efficient sparse matrix-vector multiplication on gpus. In *2013 42nd International Conference on Parallel Processing*, pages 11–20, 2013. doi: 10.1109/ICPP.2013.10.
- [21] Youcef Saad. SPARSKIT: a basic tool kit for sparse matrix computations - version 2, 1994.
- [22] Richard Vuduc, James Demmel, and Katherine Yelick. OSKI: A library of automatically tuned sparse matrix kernels. *Journal of Physics Conference Series*, 16:521–530, 01 2005. doi: 10.1088/1742-6596/16/1/071.
- [23] Richard W. Vuduc and Hyun-Jin Moon. Fast sparse matrix-vector multiplication by exploiting variable block structure. In *Proceedings of the First International Conference on High Performance Computing and Communications*, HPCC'05, page 807–816, Berlin, Heidelberg, 2005. Springer-Verlag. ISBN 3540290311.
- [24] Richard Wilson Vuduc and James W. Demmel. *Automatic Performance Tuning of Sparse Matrix Kernels*. PhD thesis, 2003. AAI3121741.
- [25] F. Vázquez, G. Ortega, J.J. Fernández, and E.M. Garzón. Improving the performance of the sparse matrix vector product with gpus. In *2010 10th IEEE International Conference on Computer and Information Technology*, pages 1146–1151, 2010. doi: 10.1109/CIT.2010.208.
- [26] Samuel Williams, Andrew Waterman, and David Patterson. Roofline: An insightful visual performance model for multicore architectures. *Commun. ACM*, 52(4):65–76, apr 2009. ISSN 0001-0782.